DALTON
FULL PAPER

New red–orange phosphorescent/electroluminescent cycloplatinated complexes of 2,6-bis(2′-indolyl)pyridine †

Qinde Liu,[a] Lisa Thorne,[a] Igor Kozin,[a] Datong Song,[a] Corey Seward,[a] Marie D'Iorio,[b] Ye Tao *[b] and Suning Wang *[a]

[a] *Department of Chemistry, Queen's University, Kingston, Ontario, K7L 3N6, Canada*
[b] *Institute for Microstructural Science, National Research Council, Ottawa, K1A 0R6, Canada*

Received 25th February 2002, Accepted 11th June 2002
First published as an Advance Article on the web 18th July 2002

Three novel cyclometalated complexes of 2,6-bis(2′-indolyl)pyridine (H_2BIP), Pd(BIP)(Py) (Py = pyridine) (**1**), Pt(BIP)(SMe_2) (**2**) and Pt(BIP)(Py) (**3**) have been synthesized and characterized structurally. The Pd and Pt centers in these compounds are four-coordinate with a square planar geometry. The BIP ligand acts as a tridentate chelate to the metal center, and the dimethyl sulfide and the pyridine ligand bind to the metal center as terminal ligands. Compound **1** has no luminescence. Compounds **2** and **3** display bright orange luminescence either at 77 K in a frozen CH_2Cl_2 solution or at ambient temperature in a polymer matrix (*e.g.* poly(carbonate) or PVK). The emission maxima for **2** and **3** in the frozen CH_2Cl_2 solution are at λ = 572 and 589 nm, respectively. The emission spectra of **2** and **3** in the polymer matrix are very similar with λ_{max} = 585 nm. The luminescence of **2** and **3** is phosphorescent as supported by the emission lifetimes of **2** (94(1) μs in CH_2Cl_2 at 77 K, 22.1(1) μs in poly(carbonate) at 298 K) and **3** (44(1) μs in CH_2Cl_2 at 77 K, 19(1) μs in poly(carbonate) at 298 K). Based on the luminescence properties of the free ligand and the results of molecular orbital calculations, we propose that the luminescence of **2** and **3** is most likely due to a $\pi \longrightarrow \pi^*$ transition with a significant d_π orbital contribution from the Pt(II) center to the π level. Electroluminescent devices using compound **3** as the emitter and PVK as the host and hole transport material have been fabricated successfully.

Introduction

Square-planar platinum complexes represent an important class of luminophores in inorganic photochemistry.[1] They have potential applications in many fields such as photosensitization,[2] chemical sensing,[3] and supramolecular photochemistry.[4] Many types of chelate ligands have been used to synthesize planar cycloplatinated or cyclopalladated complexes, such as 2,2′:6′,2″-terpyridine,[5] 6-phenyl-2,2′-bipyridine (pbpy),[6] 1,3-di(2-pyridyl)benzene,[7] 2,6-diphenylpyridine,[8] 2-phenyl-6-(2-thienyl)pyridine, and 2,6-bis(2-thienyl)pyridine.[9] In the above compounds, such as [Pt(pbpy)X] (X = Cl, PR_3, CH_3CN, pyrazole, NH_2R, pyridine), the metal ion is coordinated by an ancillary ligand X in addition to the chelate ligand. Recently Thompson, Forrest and co-workers have demonstrated that red phosphorescent Pt(II) porphyrin compounds can be used effectively as red emitters in organic light-emitting devices (OLEDs).[10a–c] Thompson and Forrest's work represents the first example of phosphorescent coordination compounds as emitters in electroluminescent devices. Using phosphorescent compounds as emitters in OLEDs has attracted much attention from both research institutions and industrial sectors because of their potential in the enhancement of overall device efficiency.[10]

In order for a phosphorescent compound to be useful in OLEDs, it must have a reasonably bright phosphorescent emission with a relatively short decay lifetime, in addition to being thermally and chemically stable and sublimable — common criteria for small molecules in OLEDs. As demonstrated by Thompson and Forrest's team, luminescent Pt(II) complexes are an attractive class of molecules as potential phosphorescent emitters in OLEDs because the Pt(II) ion displays a strong spin–orbit coupling that promotes the mixing of singlet and triplet states, thus effectively enhancing the phosphorescent emission efficiency and shortening the decay lifetime. Although luminescent Pt(II) complexes are abundant, except the porphyrin complexes, examples of Pt(II) compounds that have been demonstrated to be useful for electroluminescent applications are still scarce. Thompson and Forrest's work inspired us to search for new luminescent Pt(II) compounds that have features similar to those of Pt(II) porphyrin compounds, *i.e.* neutral molecules with nitrogen donor atoms only. Two ligand systems investigated by our group for cycloplatinated compounds are based on substituted pyridine (**A** and **B**). Ligands **A** and **B** can function as a dianionic tridentate ligand to the Pt(II) center, which in combination with a neutral ancillary ligand such as pyridine could lead to the formation of a neutral Pt(II) molecular compound that is surrounded by nitrogen donor atoms only. We have been able to synthesize Pt(II) complexes with ligand **A**, 2,6-bis(2-indolyl)pyridine (H_2BIP) successfully. Attempts to synthesize Pt(II) complexes with ligand **B**, 2,6-bis(2,7-azaindolyl)pyridine, have not been successful. For comparison purposes, we also studied the analogous complex of Pd(II). The results of our investigation on complexes of H_2BIP with Pt(II) and Pd(II) and their luminescent/electroluminescent properties are presented herein.

Experimental

Materials

All starting materials were analytical reagents and were used without further purification. Potassium tetrachloroplatinate and bis(pyridine)dichloropalladium were purchased from Fluka and the other starting materials were obtained from Aldrich. PVK and poly(carbonate) polymers were obtained from Aldrich. All solvents used in syntheses and spectroscopic

† Electronic supplementary information (ESI) available: the structure of the third independent molecule in the crystal lattice of **3** and MO diagrams for compounds **1**–**3**. See http://www.rsc.org/suppdata/dt/b2/b201951e/

 DOI: 10.1039/b201951e

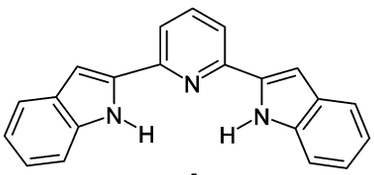

A

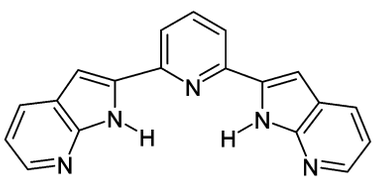

B

measurements were purified according to the literature methods. 2,6-Bis(2-indolyl)pyridine and $Pt_2(CH_3)_4(S(CH_3)_2)_2$ were synthesized according to previously reported methods.[11,12]

Measurements

Elemental analyses of C, H, and N were performed by the Canadian Microanalytical Service, Ltd., Delta, British Columbia. ^{1}H NMR spectra were measured on a Bruker Advance 400 MHz spectrometer. Excitation and emission spectra were obtained with a Photon Technologies International Quanta-Master Model C-60 spectrometer under a nitrogen atmosphere. Emission lifetime was measured on a Photon Technologies International Phosphorescent lifetime spectrometer, Time Master C-631F equipped with a Xenon flash lamp and digital emission photon multiplier tube using a band pathway of 5 nm for excitation and 2 nm for emission. All samples used for low-temperature emission spectroscopy were prepared by dissolving complexes in dichloromethane, which forms yellow glasses at 77 K. All samples for room temperature measurements were obtained as follows: complexes and poly(carbonate) (or PVK) were dissolved in dichloromethane, then several drops of solution were applied on a piece of glass by spin cast to produce thin yellow films.

Synthesis of Pd(BIP)Py (1)

2,6-Bis(2-indolyl)pyridine (0.14 g, 0.45 mmol) was dissolved in 15 mL of anhydrous THF. The solution was cooled to −78 °C with a dry ice–acetone bath. Then 0.45 mL of 2.0 M butyllithium solution in cyclohexane was added slowly. After being stirred for 30 min at −78 °C, 10 mL of THF solution containing 0.15 g (0.45 mmol) of $Pd(Py)_2Cl_2$ was added. The solution was stirred for 30 min and allowed to warm up to ambient temperature. The reaction mixture was stirred for another 2 h. All the solvent was removed under vacuum, and the residue was dissolved in 10 mL of dichloromethane. After a few days of standing at ambient temperature, dark red crystalline solid of **1** was obtained (23% yield). Anal. calc. for $C_{26}H_{18}N_4Pd\cdot 1/3CH_2Cl_2$: C 60.66, H 3.58, N 10.75. Found: C 60.49, H 3.63, N 10.91%. ^{1}H NMR ($CDCl_3$, 400 MHz): δ 9.17 (dd, 2H, J_1 = 4.8, J_2 = 1.6 Hz, py), 8.12 (tt, 1H, J_1 = 7.6, J_2 = 1.6 Hz, py), 7.47–7.57 (m, 5H, indolyl and py), 7.12 (d, 2H, J = 8.0 Hz, indolyl), 6.92 (s, 2H, indolyl), 6.84 (ddd, 2H, J_1 = 8.0, J_2 = 6.8, J_3 = 0.8 Hz, indolyl), 6.69 (ddd, J_1 = 8.4, J_2 = 6.8, J_3 = 1.2 Hz, indolyl), 5.42–5.45 (dd, 2H, J_1 = 8.0, J_2 = 0.8 Hz, indolyl).

Synthesis of Pt(BIP)(S(Me)$_2$) (2)

$Pt_2Me_4(SMe_2)_2$ (84 mg, 0.15 mmol) and H_2BIP (90 mg, 0.29 mmol) were mixed and dissolved in anhydrous THF. The solution was stirred for 2 days at room temperature. The solvent was removed under vacuum, and the solid was dissolved in dichloromethane. After a few days of standing at ambient temperature, dark red crystals of **2** were deposited and collected (21% yield). Anal. calc. for $C_{23}H_{19}N_3PtS$: C 48.93, H 3.39, N 7.44. Found: C 48.40, H 3.33, N 7.19%. ^{1}H NMR ($CDCl_3$, 400 MHz): δ 7.78 (t, 1H, J = 8.0 Hz, py), 7.69 (d, 2H, J = 8.4 Hz, py), 7.60 (d, 2H, J = 8.4 Hz, indolyl), 7.42 (d, 2H, J = 7.6 Hz, indolyl), 7.14 (t, 2H, J = 8.0 Hz, indolyl), 7.07 (s, 2H, indolyl), 6.98 (t, 2H, J = 7.6 Hz, indolyl), 3.16 (s, with satellites, 6H, J_{Pt-H} = 42.4 Hz, methyl).

Synthesis of Pt(BIP)Py (3)

Complex **2** (30 mg, 0.053 mmol) was dissolved in 5 mL of dichloromethane. After being stirred for 30 min, 0.2 mL of pyridine solution in dichloromethane (0.024 g mL^{-1}, 0.061 mmol) was added. The solution was stirred for 2 h and then allowed to stand at ambient temperature. Dark red crystals were collected after 3 days (65% yield). Anal. calc. for $C_{26}H_{18}N_4Pt$: C 53.70, H 3.12, N 9.63. Found: C 54.08, H 2.97, N 9.75%. ^{1}H NMR ($CDCl_3$, 400 MHz): δ 9.20 (dd, 2H, J_1 = 6.4, J_2 = 1.2 Hz, py), 7.98 (tt, 1H, J_1 = 7.6, J_2 = 1.6 Hz, py), 7.54 (d, 2H, J_1 = 8.0 Hz, py), 7.37 (t, 1H, J_1 = 8.0 Hz, py), 7.22 (dd, 2H, J_1 = 7.6, J_2 = 6.4 Hz, py), 7.00 (d, 2H, J_1 = 8.0 Hz, indolyl), 6.86 (ddd, 2H, J_1 = 8.0, J_2 = 6.8, J_3 = 0.8 Hz, indolyl), 6.64 (s, 2H, indolyl), 6.68 (ddd, 2H, J_1 = 8.0, J_2 = 6.8, J_3 = 1.2 Hz, indolyl), 5.46 (dd, 2H, J_1 = 8.0, J_2 = 0.8 Hz, indolyl).

Fabrication of electroluminescent devices

The EL devices using compound **3** as the emitting layer were fabricated on an indium tin oxide (ITO) substrate, which was cleaned by an ultraviolet ozone cleaner immediately before use. The solution for spin-coating was made up of 10 g chlorobenzene, 100 mg of PVK, and 20 mg of compound **3** (1 wt% solution, 20% doped Pt-complex). This solution was stirred for about 2 h, then filtered to remove any undissolved material or insoluble impurities. It was then spin-cast onto an ITO glass at 1600 rpm for about 45 seconds, producing a film about 400–500 Å thick. The electron transport material PBD (2-(4-biphenyl)-5-(4-*tert*-butylphenyl)-1,3,4-oxadiazole) layer was deposited *in vacuo*. The cathode composed of LiF and Al was deposited on the substrate by conventional thermal vacuum deposition. A single-layer device with the structure ITO/PVK + **3** (~50 nm)/LiF (1.5 nm)/Al (150 nm) and a double-layer device with the structure ITO/PVK + **3** (~50 nm)/PBD (30 nm)/LiF (1.5 nm)/Al (150 nm) were fabricated. The active device area is 1.0 × 5.0 mm^2. The current/voltage characteristics were measured using a Keithley 238 Source Measure Unit. The EL spectra and the luminance for the devices were measured by using a Photo Research-650 Spectra Colorimeter.

X-Ray crystal structure determination

The diffraction experiments were carried out on a Siemens P4 diffractometer with a Bruker CCD 1000 detector and graphite-monochromated Mo-Kα radiation, operating at 50 kV and 35 mA at 23 °C. The software used were SMART[13] for collecting frames of data, indexing reflections, and determination of lattice parameters; SAINT[14] for integration of intensities of reflections and scaling; SADABS[14] for empirical absorption corrections; and SHELXTL[15] for space group determination and structure solutions and least-squares refinements on F^2. The crystals were mounted at the end of glass fibers and used for the diffraction experiments. All structures were solved by direct methods. Compound **3** is disordered. The systematic absences of **3** agree with both *C*2 and *C*2/*m* space groups. The *C*2/*m* space group was chosen based on statistical analysis and the successful solution and refinement of the structure. There are three independent molecules in the asymmetric unit, two of which are at the inversion center sites and the remaining one is at the mirror plane site. Although the disordering of **3** was

Table 1 Crystal data for **1**, **2** and **3**

	1	**2**	**3**
Formula	$C_{26}H_{18}N_4Pd$	$C_{23}H_{19}N_3PtS$	$C_{26}H_{18}N_4Pt$
Color	Dark red	Dark red	Dark red
FW	492.84	564.56	581.53
Crystal system	Monoclinic	Monoclinic	Monoclinic
Space group	*I*2/*a*	*I*2/*a*	*C*2/*m*
a/Å	25.968(4)	25.271(6)	19.264(3)
b/Å	6.0223(9)	5.9002(16)	17.951(3)
c/Å	27.835(4)	27.604(8)	14.900(2)
β/°	108.531(3)	109.011(5)	124.408(2)
V/Å^3	4127.3(11)	3891.4(18)	4251.3(10)
Z	8	8	8
T/K	295	295	295
μ/mm^{-1}	0.920	7.333	6.622
F(000)	1984	2176	2240
λ/Å	0.71073	0.71013	0.71013
Reflections collected	14491	13326	15589
Independent reflections	4927	4634	5143
Parameters	352	253	273
Final R [$I > 2\sigma(I)$]	R_1[a] = 0.0377	R_1 = 0.0787	R_1 = 0.0883
	wR_2[b] = 0.0482	wR_2 = 0.1602	wR_2 = 0.1789
R (all data)	R_1 = 0.1156	R_1 = 0.1190	R_1 = 0.1002
	wR_2 = 0.0594	wR_2 = 0.1680	wR_2 = 0.1824

[a] $R_1 = \Sigma||F_o|^2 - |F_c|^2|/\Sigma|F_o|^2$. [b] $wR_2 = [\Sigma w[(F_o^2 - F_c^2)^2]/\Sigma[w(F_o^2)^2]]^{1/2}$; $w = 1/[\sigma^2(F_o^2) + (0.075P)^2]$, where $P = [\mathrm{Max}(F_o^2,0) + 2F_c^2]/3$.

modeled successfully, the quality of the crystal data and refinements were definitely affected by the disordering. The positions of all hydrogen atoms in **1** and **2**, and some of the hydrogen atoms on non-disordered carbon atoms in **3** were calculated and refined using a riding model (The coordinates of the hydrogen atoms ride on the coordinates of the carbon atoms they are attached to.). The isotropic thermal parameters of the hydrogen atoms were fixed at 1.2 times those of the carbon atoms they are attached to. Details of the data collections and refinements are listed in Table 1.

CCDC reference numbers 180226–180228.

See http://www.rsc.org/suppdata/dt/b2/b201951e/ for crystallographic data in CIF or other electronic format.

Results and discussion

Syntheses and structures

Compound **1**, Pd(BIP)(Py) was obtained readily from the reaction of Li_2(BIP) with $Pd(Py)_2Cl_2$ in an approximate 3 : 1 ratio (The excess ligand used is necessary to ensure that **1** is obtained in reasonable yield.). Repeated attempts to obtain the Pt(II) analogue, Pt(BIP)(Py), **3**, by using the same method, was however unsuccessful. The best way to synthesize compound **3**, we have found, is to replace the labile dimethylsulfide ligand in Pt(BIP)(SMe_2), **2** by a pyridine ligand. Compound **2** can be obtained in modest yield from the reaction of $Pt_2Me_4(SMe_2)_2$ with H_2BIP in THF. The synthetic routes for compounds **1**–**3** are summarized in Scheme 1. All three compounds are stable in solution and the solid state under air and have been fully characterized by ^{1}H NMR, elemental and X-ray diffraction analyses.

The molecular structure of **1** is shown in Fig. 1. The four Pd–N bond lengths (see Table 2) range from 1.962(3) to 2.040(3) Å, typical for Pd(II) complexes.[16] The geometry around the Pd center is however significantly distorted from an ideal square plane as indicated by the bond angles of N(1)–Pd(1)–N(3) (161.52(12)°) and N(2)–Pd(1)–N(4) (172.94(13)°). The geometric constraint imposed by the BIP ligand is believed to be responsible for such distortion. The pyridine ligand is nearly perpendicular to the BIP ligand, attributable to steric interactions between these two ligands. In the crystal lattice, molecules of **1** stack like a ladder along the *c* axis with the Pd–Pd separation distance being 6.002(1) Å.

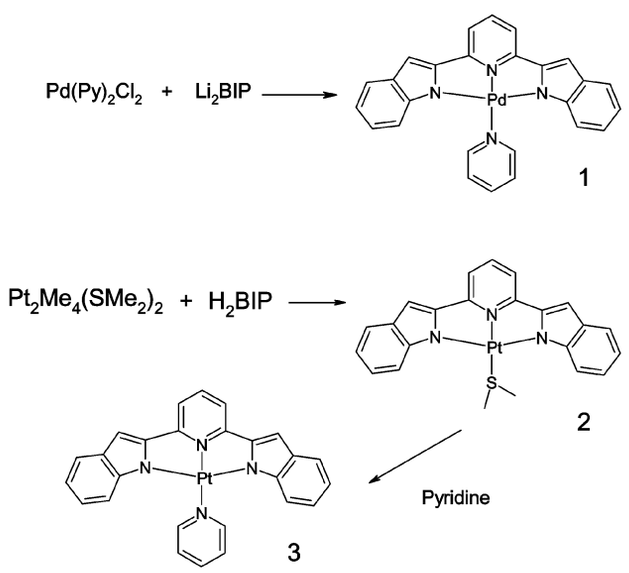

Scheme 1

The molecular structure of **2** is shown in Fig. 2. The Pt–N bond lengths in **2** range from 1.971(9) to 2.070(12) Å. The Pt(1)–S(1) distance of 2.284(3) Å is comparable to previously known Pt–S bond lengths.[17] As observed in **1**, the Pt(II) center in **2** also shows considerable distortion from an ideal square plane as evident by the N(3)–Pt(1)–N(1) bond angle of 160.3(4)° and the N(2)–Pt(1)–S(1) bond angle of 162.8(3)°. The sulfur atom is at 0.727 Å above the Pt(1)N(1)N(2)N(3) plane while the two methyl groups in complex **2** are located above and below the plane, respectively. Compounds **1** and **2** belong to the same monoclinic space group *I*2/*a* with similar unit cell dimensions. Compound **2** stacks like a ladder along the *c* axis in the crystal lattice in the same manner as compound **1** with the Pt–Pt separation being 5.900(2) Å.

Compound **3**, albeit an analogue of **1**, belongs to the monoclinic space group *C*2/*m* with a very different molecular packing in the crystal lattice from those of **1** and **2**. There are three independent molecules in the asymmetric unit, each one of which sits on a symmetry element (two sit on inversion centers and the third one possesses a mirror plane symmetry). Due to the crystallographically imposed symmetry, all three molecules

Table 2 Selected bond lengths (Å) and angles (°) for **1**–**3**

Complex **1**			
Pd(1)–N(1)	2.007(3)	Pd(1)–N(2)	1.962(3)
Pd(1)–N(3)	2.009(3)	Pd(1)–N(4)	2.040(3)
N(2)–Pd(1)–N(1)	80.52(13)	N(2)–Pd(1)–N(3)	81.11(13)
N(1)–Pd(1)–N(3)	161.52(12)	N(2)–Pd(1)–N(4)	172.94(13)
N(1)–Pd(1)–N(4)	100.03(12)	N(3)–Pd(1)–N(4)	98.44(12)
Complex **2**			
Pt(1)–N(1)	2.070(12)	Pt(1)–N(2)	1.971(9)
Pt(1)–N(3)	2.043(10)	Pt(1)–S(1)	2.284(3)
N(2)–Pt(1)–N(3)	79.7(4)	N(2)–Pt(1)–N(1)	80.9(4)
N(3)–Pt(1)–N(1)	160.3(4)	N(2)–Pt(1)–S(1)	162.8(3)
N(3)–Pt(1)–S(1)	94.4(3)	N(1)–Pt(1)–S(1)	105.3(3)
Complex **3** (one of the independent molecules)			
Pt(1)–N(2)	1.986(17)	Pt(1)–N(3)	2.03(2)
Pt(1)–N(1)	2.041(15)		
N(2)–Pt(1)–N(1)	179.2(7)	N(1)–Pt(1)–N(3)	99.1(5)
N(2)–Pt(1)–N(3)	80.9(5)	N(3)–Pt(1)–N(3A)	161.7(10)

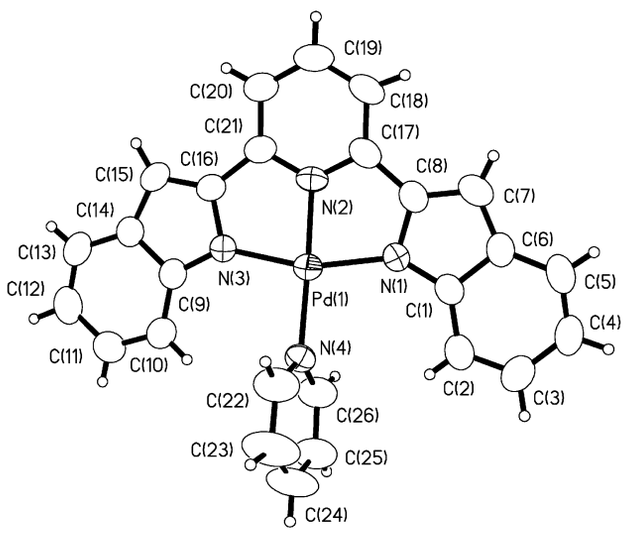

Fig. 1 The molecular structure of **1** with labeling schemes and 50% probability thermal ellipsoids.

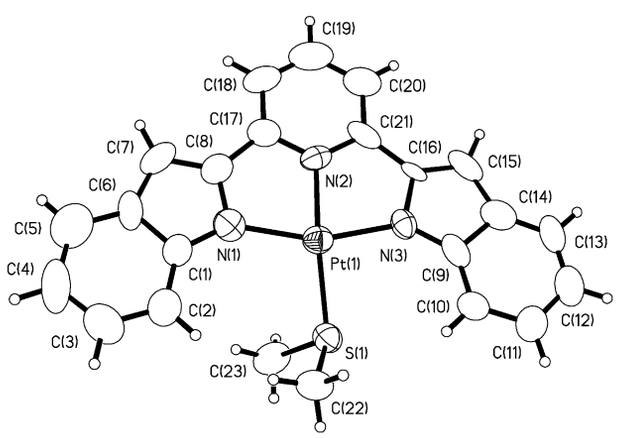

Fig. 2 The molecular structure of **2** with labeling schemes and 50% probability thermal ellipsoids.

are disordered. Fig. 3 shows the structures of two of the disordered molecules (one sits on the inversion center and the other on a mirror plane). Although the structural parameters for **3** are not well defined due to disordering, the crystal data established unequivocally that the molecular structure of **3** resembles that of **1**. Molecules of **3** stack directly on top of each

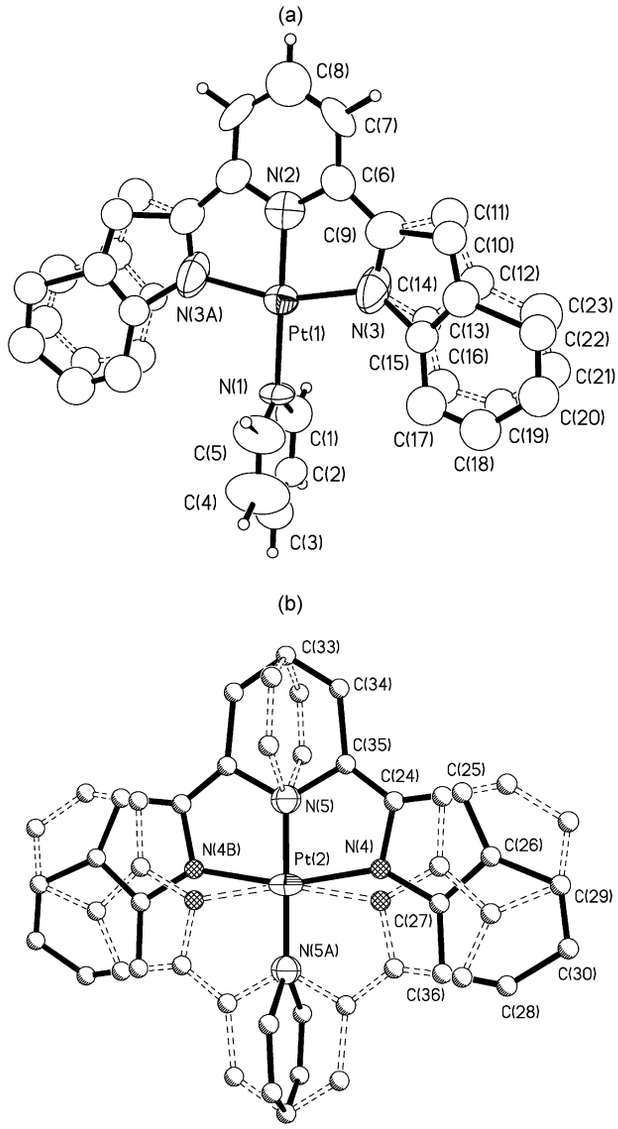

Fig. 3 (a) A diagram showing the disordered structure on a mirror plane symmetry of one of the independent molecules of **3** in the crystal lattice with labeling schemes and 50% probability thermal ellipsoids. (b) A diagram showing the disordered structure on 2/*m* symmetry of the second independent molecule of **3** in the crystal lattice with labeling schemes and 50% probability thermal ellipsoids. The structure of the third independent molecule is similar to that shown in Fig. 3a.

other and form extended linear columns in the crystal lattice with Pt–Pt separation distances being 4.08(1) Å. There is extensive intermolecular π–π stacking among the BIP ligands and among the pyridine ligands. Besides porphyrin complexes, neutral Pd(II) and Pt(II) complexes that are surrounded only by nitrogen donor atoms are rare. Compounds **1** and **3** are among the first examples of such rare neutral Pd(II) and Pt(II) complexes.

Photoluminescent properties of 1–3

The neutral H_2BIP ligand is a bright blue emitter with an emission maximum at $\lambda = 401$ nm in solution and $\lambda = 430$ nm in the solid state at ambient temperature. At 77 K, the H_2BIP molecule displays an intense fluorescent emission band at $\lambda =$ 387nm in CH_2Cl_2 solution. Using a time-resolved phosphorescence spectrometer, a weak phosphorescent emission band at 571 nm with a decay lifetime of 63.9(2) μs was observed for H_2BIP in CH_2Cl_2 at 77 K. In contrast, the Pd(II) and Pt(II) complexes of BIP show quite different luminescent properties. No luminescence was observed for compound **1** in solution or the solid state at 77 K or ambient temperature. Although no

Table 3 UV-Vis absorption data (CH_2Cl_2, 298 K) for H_2BIP and compounds **1**–**3**

Compound	Absorption/nm (ε/M^{-1} cm^{-1})
H_2BIP	322 (27900), 354 (33400)
1	340 (29340), 414 (25980), 436 (25140)
2	336 (37250), 350 (38780), 426 (30600)
3	350(27400), 418 (21800)

luminescence was observed for compounds **2** and **3** in the solid state, the frozen solutions of **2** and **3** display bright red–orange luminescence at 77 K with emission maxima at λ = 570 and 588 nm, respectively. The decay lifetime of the orange emission from **2** and **3** in CH_2Cl_2 at 77 K was determined to be 94(1) and 43.6(1) μs, respectively, indicative of phosphorescent emission. The excitation/UV-Vis spectra of compounds **2** and **3** are essentially identical. The UV-Vis, excitation and emission spectra of **2** are shown in Fig. 4. The emission spectra of **3** are shown in Fig. 5. Tables 3 and 4 summarize UV-Vis, excitation and emission data for H_2BIP and compounds **1**–**3**. The fact that SMe_2 and the pyridine ligand do not cause a significant difference in the excitation energy of **2** and **3** and that the emission bands of **2** and **3** match approximately the phosphorescent emission band of H_2BIP led us to believe that the observed emission is most likely due to the BIP ligand-based transitions.

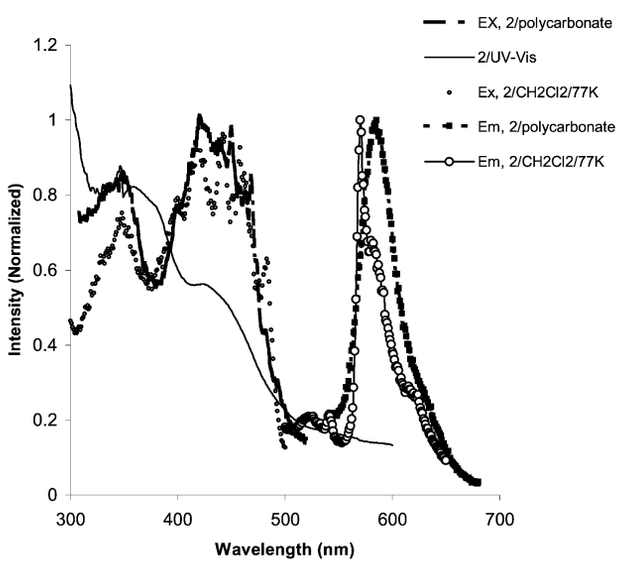

Fig. 4 UV-Vis, excitation and emission spectra of **2**.

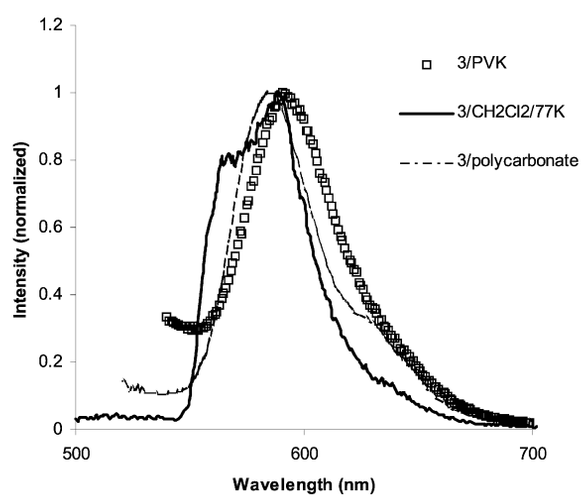

Fig. 5 Photoluminescent emission spectra of **3**.

In order to understand the nature of luminescence displayed by **1**–**3**, we carried out molecular orbital calculations for compounds **1**–**3** using extended Huckel methods.[19] The molecular geometry was established by using the crystallographic coordinates of compounds **1**–**3**. Molecular orbital calculations performed for compounds **1**–**3** show that both HOMO and LUMO levels for compounds **2** and **3** are π orbitals of the BIP ligand with a considerable contribution from the d_π orbital of the Pt(II) center. The energy gap between HOMO (−11.65 eV for **2** and −11.69 eV for **3**) and LUMO (−9.52 eV for **2** and −9.50 eV for **3**) of compounds **2** and **3** is similar. The second HOMO that is very close in energy to the HOMO consists of mostly the d_{z^2} (d_σ) orbital of the Pt(II) center in **2** and **3**. Therefore, we suggest that the observed red–orange emission of **2** and **3** is most likely due to a $\pi \longrightarrow \pi^*$ transition centered on the BIP ligand with a considerable d_π contribution from the Pt(II) center. The fact that the orange–red phosphorescent emission in **2** and **3** is much brighter than that of the free H_2BIP ligand (not observable by eye but detectable by time-resolved spectroscopy) and that the intense fluorescent emission band displayed by the H_2BIP molecule was not detected for **2** and **3** at ambient temperature or at 77 K appears to support the idea that the ^1S to ^1T inter-system crossing in **2** and **3** is very efficient, attributable to spin–orbit coupling promoted by the Pt(II) center.[18,20] We believe that chelation of the BIP ligand to the Pt(II) center also contributes to the enhancement of the phosphorescent emission by increasing the rigidity of the ligand, thus reducing the loss of energy by thermal vibrational decay.[21] For compound **1**, the HOMO level consists of nearly entirely the d_{z^2} (d_σ) orbital of the Pd(II) center while the LUMO level is similar to those of **2** and **3** but with much less contribution from the d_π orbital of the Pd(II) center.

The absence of emission from compound **1** is not surprising since it is well-known that most Pd(II) complexes are not emissive. The absence of emission from **2** and **3** at ambient temperature in solution and the solid state can be attributed to collisional quenching by the solvent molecules in solution[21] and intermolecular interactions in the crystal lattice, commonly observed for phosphorescent metal compounds. If, however, compounds **2** and **3** can be doped into a polymer matrix, collisional quenching and intermolecular interactions could be greatly reduced, hence it may be possible to observe the phosphorescent emission at ambient temperature. Indeed, we have observed that compound **2** or **3** doped polymer films (poly(carbonate) or PVK) produce bright orange–red emission when irradiated by UV light at ambient temperature. The excitation spectra of the doped polymer films match those of the frozen solutions of **2** and **3**. The emission spectra of **2** and **3** in poly(carbonate) films are identical with λ_{max} = 585 nm. The decay lifetimes of the emission by **2** and **3** in the polymer film are much shorter than those of the frozen solutions (11–22 μs), making it possible to use **2** and **3** as emitters in light-emitting devices where a polymer is used as a host. Doping phosphorescent emitters into a polymer matrix or a small molecule solid matrix to enhance phosphorescent emission intensity has been demonstrated by a number of research groups previously.[10]

Electroluminescence of compound 3

Two types of electroluminescent devices using compound **3** as the emitter were fabricated. The first type consists of a single-layer of compound **3** doped PVK film (20%, ~50 nm) sandwiched between an ITO anode and a LiF(1.5 nm)/Al(150 nm) cathode. The second type consists of a layer of compound **3** doped PVK film (20%, ~50 nm) and a layer of vacuum deposited PBD (2-(4-biphenyl)-5-(4-*tert*-butylphenyl)-1,3,4-oxadiazole, 30 nm) sandwiched between the ITO anode and LiF(1.5 nm)/Al(150 nm) cathode. The choice of PVK as the host material is based on the fact that PVK is an excellent hole-transport material with an emission band in the blue-region

Table 4 Phosphorescent data for H_2BIP and compounds **2** and **3**

Compound	Excitation λ_{max}/nm	Fluorescence λ_{max}/nm	Phosphorescence λ_{max}/nm	Lifetime τ/μs
H_2BIP, CH_2Cl_2, 77 K	380	400	571 (very weak)	63.9(2)
Pt(BIP)(SMe_2), CH_2Cl_2, 77 K	419	Not observed	570	94(1)
Pt(BIP)(SMe_2), poly(carbonate), RT	419	Not observed	585	22.1(1)
Pt(BIP)Py, CH_2Cl_2 at 77 K	420	Not observed	588	43.6(1)
Pt(BIP)Py in poly(carbonate), RT	420	Not observed	585	19(1)
Pt(BIP)Py in PVK, RT	420	Not observed	592	11.85(6)

that overlaps with the excitation band of compound **3**. The PL spectrum of compound **3**-doped PVK film is dominated by the emission of **3** with only a small fraction of emission (~5%) by PVK, an indication that the energy transfer from PVK to **3** is efficient. An emission band in the red–orange region was observed for both devices, which matches the PL of **3**. A weak emission band at ~400 nm due to PVK was also observed. The *L*–V-efficiency diagram of the single-layer device is shown in Fig. 6. The single-layered device is clearly not efficient. The device performance was improved dramatically when a PBD layer is included as shown by the *L*–V-efficiency characteristics of the double-layered device in Fig. 7.

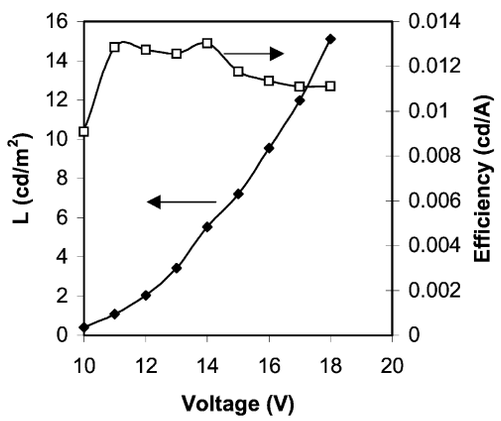

Fig. 6 *L*–V-efficiency diagram for the single-layered device of **3**.

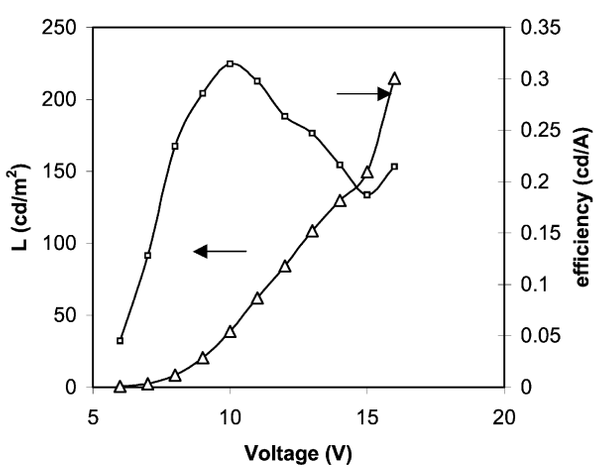

Fig. 7 *L*–V-efficiency diagram for the double-layered device of **3**.

PBD is an electron-transport material. The inclusion of the PBD layer in the double-layered device clearly facilitates the electron transport from cathode to anode, and forms a hole barrier at the PVK/PBD interface, hence improving the efficiency of the device. Use of PVK as the host/hole transport layer and PBD as the electron transport layer for phosphorescent emitters and lanthanide emitters in electroluminescent devices has been well documented previously.[20] The electroluminescent spectra of the double-layered device are shown in Fig. 8. The C.I.E. coordinates (1976 U.C.S.) are u' = 0.353,

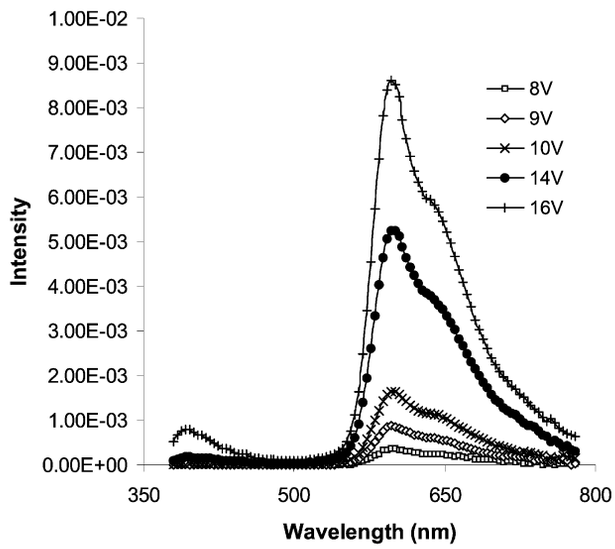

Fig. 8 EL of the double-layered device of **3**.

v' = 0.543 for the double-layered device, corresponding to the red–orange region. The highest efficiency (0.31 cd A^{-1}) for the double-layered device was achieved at 10 V and 20 mA cm^{-2}. We also attempted to use Alq_3 (Alq_3 = tris(8-hydroxyquinolinato)aluminium(III)) as the electron transport layer in the EL device. However, these devices emit a yellow–green color that is characteristic of Alq_3 and no emission band from **3** was observed. The performance of the EL device of **3** could be improved further if a small molecule host layer doped by **3** *via* vacuum deposition were employed. Unfortunately, we have not been able to sublime compound **3** without decomposition. Therefore, attempts to dope compound **3** into a solid host layer by vacuum deposition were not made. Pt(II) porphyrin compounds are the first type of Pt(II) chelate compounds that have been demonstrated to be useful phosphorescent emitters in electroluminescent devices.

In summary, a new type of Pt(II) compounds have been synthesized and demonstrated to be promising phosphorescent emitters in electroluminescent devices. Efforts are being taken to further optimize the EL devices based on compound **3** and to fabricate new EL devices using analogues of compound **3** as emitters.

Acknowledgements

We are indebted to Dr Nan Xing Hu at the Xerox Research Center of Canada for his assistance in evaluating PL properties of doped PVK films. We thank the Natural Sciences and Engineering Research Council of Canada and the Canada Foundation for Innovation for financial support.

References

1 (*a*) V. H. Houlding and V. M. Miskowski, *Coord. Chem. Rev.*, 1991, **111**, 145; (*b*) C. N. Pettijohn, E. B. Jochnowitz, B. Chuong, J. K. Nagle and A. Vogler, *Coord. Chem. Rev.*, 1998, **171**, 85; (*c*) H. Yersin, W. Humbs and J. Strasser, *Coord. Chem. Rev.*, 1997, **159**, 325;

(*d*) W. Paw, S. D. Cummings, M. A. Mansour, W. B. Connick, D. K. Gieger and R. Eisenberg, *Coord. Chem. Rev.*, 1998, **171**, 125; (*e*) J. E. McGarrah, Y. J. Kim, M. Hissler and R. Eisenberg, *Inorg. Chem.*, 2001, **40**, 4510.

2 (*a*) L. Chassot, E. Müller and A. von Zelewsky, *Inorg. Chem.*, 1984, **23**, 4249; (*b*) D. Sandrini, M. Maestri, V. Balzani, L. Chassot and A. von Zelewsky, *J. Am. Chem. Soc.*, 1987, **109**, 3107; (*c*) A. Vogler and H. Kunkely, *Coord. Chem. Rev.*, 1998, **177**, 81; (*d*) K. T. Wan, C. M. Che and K. C. Cho, *J. Chem. Soc., Dalton Trans.*, 1991, 1077; (*e*) C. M. Che, K. T. Wan, L. T. He, C. K. Poon and V. W. W. Yam, *J. Chem. Soc., Dalton Trans.*, 1989, 2011; (*f*) K. T. Wan and C. M. Che, *J. Chem. Soc., Chem. Commun.*, 1990, 140.

3 (*a*) L. Z. Wu, T. C. Cheung, C. M. Che, K. K. Cheung and M. H. H. Lam, *Chem. Commun.*, 1998, 1127; (*b*) W. W. S. Lee, K. Y. Wong and X. M. Li, *Anal. Chem.*, 1993, **65**, 255; (*c*) M. Cusumano, M. L. Di Pietro and A. Giannetto, *Inorg. Chem.*, 1999, **38**, 1754; (*d*) K. H. Wong, M. C. W. Chan and C. M. Che, *Chem. Eur. J.*, 1999, **10**, 2845.

4 (*a*) R. Ballardini, M. T. Gandolfi, V. Balzani, F. H. Kohnke and J. F. Stoddart, *Angew. Chem., Int. Ed. Engl.*, 1988, **27**, 692; (*b*) R. Ballardini, M. T. Gandolfi, L. Prodi, M. Ciano, V. Balzani, F. H. Kohnke, H. Shahriari-Zavareh, N. Spencer and J. F. Stoddart, *J. Am. Chem. Soc.*, 1989, **111**, 7072; (*c*) M. C. Tse, K. K. Cheung, M. C. W. Chan and C. M. Che., *Chem. Commun.*, 1998, 2295; (*d*) C. W. Chan, T. F. Lai, C. M. Che and S. M. Peng, *J. Am. Chem. Soc.*, 1993, **115**, 11245.

5 (*a*) S. A. Ross, G. Lowe and D. J. Watkin, *Acta Crystallogr., Sect. C*, 2001, **57**, 275; (*b*) S. Bonse, J. M. Richards, S. A. Ross, G. Lowe and R. L. Krauth-Siegel, *J. Med. Chem.*, 2000, **43**, 4812; (*c*) R. Romeo, L. M. Scolaro, M. R. Plutino and A. Albinati, *J. Organomet. Chem.*, 2000, **593**, 403; (*d*) V. W. W. Yam, K. P. L. Tang, K. M. C. Wong, C. C. Ko and K. K. Cheung, *Inorg. Chem.*, 2001, **40**, 571.

6 (*a*) E. C. Constable, R. P. G. Henney, T. A. Leese and D. A. Tocher, *J. Chem. Soc., Chem. Commun.*, 1990, 513; (*b*) H. Q. Liu, T. C. Cheung and C. M. Che, *Chem. Commun.*, 1996, 1039; (*c*) E. C. Constable, R. P. G. Henney, T. A. Leese and D. A. Tocher, *J. Chem. Soc., Dalton Trans.*, 1990, 443; (*d*) F. Neve and A. Crispini, *Inorg. Chem.*, 1997, **36**, 6150; (*e*) Y. G. Ma, T. C. Cheung, C. M. Che and J. C. Shen, *Thin Solid Films*, 1998, **333**, 224; (*f*) T. C. Cheung, K. K. Cheung, S. M. Peng and C. M. Che, *J. Chem. Soc., Dalton Trans.*, 1996, 1645; (*g*) Y. Jahng and J. G. Park, *Inorg. Chim. Acta*, 1998, **267**, 265; (*h*) J. H. K. Yip, Suwarno and J. J. Vittal, *Inorg. Chem.*, 2000, **39**, 3537; (*i*) S. W. Lai, M. C. W. Chan, T. C. Cheung, S. M. Peng and C. M. Che, *Inorg. Chem.*, 1999, **38**, 4046; (*j*) S. W. Lai, M. C. W. Chan, K. K. Cheung and C. M. Che, *Organometallics*, 1999, **18**, 3327.

7 D. J. Cárdenas and A. M. Echavarren, *Organometallics*, 1999, **18**, 3337.

8 (*a*) M. Maestri, *Coord. Chem. Rev.*, 1991, **111**, 117; (*b*) G. W. V. Cave, N. W. Alcock and J. P. Rourke, *Organometallics*, 1999, **18**, 1801; (*c*) G. W. V. Cave, F. P. Franizzi, R. J. Deeth, W. Errington and J. P. Rourke, *Organametallics*, 2000, **19**, 1355.

9 E. C. Constable, R. P. G. Henney and D. A. Tocher, *J. Chem. Soc., Dalton Trans.*, 1992, 2467.

10 (*a*) M. A. Baldo, D. F. O'Brien, Y. You, A. Shoustikov, S. Sibley, M. E. Thompson and S. R. Forrest, *Nature*, 1998, **395**, 151; (*b*) R. C. Kwong, S. Sibley, T. Dubovoy, M. Baldo, S. R. Forrest and M. E. Thompson, *Chem. Mater.*, 1999, **11**, 3709; (*c*) R. C. Kwong, S. Lamansky and M. E. Thompson, *Adv. Mater.*, 2000, **12**, 1134; (*d*) S. Lamansky, P. Djurovich, D. Murphy, F. Abdel-Razzaq, H. E. Lee, C. Adachi, P. E. Burrows, S. R. Forrest and M. E. Thompson, *J. Am. Chem. Soc.*, 2001, **123**, 4304; (*e*) W. Lu, B. X. Mi, M. C. W. Chan, Z. Hui, N. Zhu, S. T. Lee and C. M. Che, *Chem. Commun.*, 2002, 206.

11 R. P. Thummel and V. Hegde, *J. Org. Chem.*, 1989, **54**, 1720.

12 G. S. Hill, M. J. Irwin, C. J. Levy, L. M. Rendina and R. J. Puddephatt, *Inorg. Synth.*, 1998, **32**, 149.

13 SMART for Windows NT v5.050, Bruker AXS Inc., Madison, WI, 1998.

14 SAINT^{+} for NT™ v5.00, Bruker AXS Inc., Madison, WI, 1998.

15 SHELXTL NT v. 5.1, Bruker AXS Inc., Madison, WI, 1998.

16 (*a*) D. J. Cárdenas and A. M. Echavarren, *Organometallics*, 1999, **18**, 3337; (*b*) D. Song, Q. Wu, A. Hook, I. Kozin and S. Wang, *Organometallics*, 2001, **20**, 4683.

17 D. P. Bancroft, F. A. Cotton, L. R. Falvello and W. Schwotzer, *Inorg. Chem.*, 1986, **25**, 763.

18 R. S. Drago, *Physical Methods in Chemistry*, W. B. Saunders Company, Philadelphia, 1977, ch. 5.

19 (*a*) C. Mealli and D. M. Proserpio, *J. Chem. Educ.*, 1990, **67**, 399; (*b*) J. H. Ammeter, H. B. Bürgi, J. L. Thibeault and R. Hoffmann, *J. Am. Chem. Soc.*, 1978, **100**, 3686; (*c*) P. J. Hay, J. C. Thibeault and R. Hoffmann, *J. Am. Chem. Soc.*, 1975, **97**, 4884.

20 (*a*) J. Wang, R. Wang, J. Yang, Z. Zheng, M. D. Carducci, T. Cayou, N. Peyghambarian and G. E. Jabbour, *J. Am. Chem. Soc.*, 2001, **123**, 6179; (*b*) C. L. Lee, K. B. Lee and J. K. Kim, *Appl. Phys. Lett.*, 2000, **77**, 2280; (*c*) M. J. Yang and T. Tsutsui, *Jpn. J. Appl. Phys.*, 2000, **39**, L828; (*d*) M. R. Robinson, M. B. O'Regan and G. C. Bazan, *Chem. Commun.*, 2000, 1645.

21 (*a*) J. R. Lakowicz, *Principles of Fluorescence Spectroscopy*, 2nd edn., Kluwer Academic, New York, 1999; (*b*) J. D. Ingle, Jr. and S. R. Crouch, *Spectrochemical Analysis*, Prentice Hall, New Jersey, 1988, ch. 12.